(Received 18 July 2023, Accepted 20 November 2023, Scheduled 28 November 2023)

Skin Sarcoma Detection by Antenna Resonance Scale

Dozohoua Silue*, Fethi Choubani, and Mondher Labidi

Innov'Com Laboratory, SUP'COM, University of Carthage, Tunis, Tunisia

ABSTRACT: In this paper, a small antenna is proposed to diagnose skin sarcoma from the embryonic stage to the metastasis stage. The prototype consists of a new antenna structure with a surface of $31.3 \times 15.65\,\text{mm}^2$ and a 35 µm copper sheet engraved on a 1.6 mm FR-4 substrate. The diagnosis is based on the shift in resonance frequency when the antenna is positioned on malignant tissue. For the simulations, a three-layer body phantom (skin, fat, and muscle) and a half-sphere tumor Phantom were considered. Simulations of antenna performances showed that for a tumor of $26.17\,\text{mm}^3$, the resonance frequency decreases by 7.5 MHz. Measurements made on the prototype of the designed antenna show an adequacy between the results of the measurement and those of the simulation.

1. INTRODUCTION

Skin cancer is a form of cancer that is developing more and more due to the emergence of factors such as the aging of the population, the change in leisure habits, and the fashion for tanned skin [1]. According to [2], skin cancer is on the rise in recent years. In about 20 years, the annual number of new cases in Belgium has increased from less than 11,000 in 2004 to more than 43,000 in 2018. The skin structure is complex, and the cancers that attack it are diverse. Healthy skin (1–4 mm) mainly consists of three parts: epidermis, dermis, and hypodermis.

Depending on their location in the skin, there are several types of cancer.

- Basal cell carcinomas constitute 70% skin cancers. They develop when the keratinocytes located in the deepest layer of the epidermis (stratum basal) are altered. In their invasive state, basal cell carcinomas can reach 20 mm [3].

- Melanomas constitute about 20% of skin cancers. They arise from melanocytes and are the most serious form of skin cancer.

- Cutaneous sarcoma is a type of cancer that develops in the dermis and hypodermis. It accounts for 2% of all cases of skin cancer. The diagnosis of skin sarcoma is very complex, so it is recommended to have at least two expert opinions. The most used examination to detect a skin sarcoma is histology, which allows the tumor to be characterized by taking a sample and visually analyzing a piece of tissue (anatomopathology).

Regardless of skin cancer type, early diagnosis helps to avoid proliferation through metastasis or invasive cancer. Early detection of cancer increases the patient's chances of recovery.

In-depth knowledge of the dielectric characteristics of tissues today has facilitated the emergence of new cancer detection methods based on the analysis of these characteristics.

The dielectric properties of different tissues were analyzed by Joines and others in [4] over the 50–900 MHz band. Comparing healthy and diseased tissues, the authors observed respectively an increase in relative permittivity and conductivity of 6.4 and 3.8 S/m in malignant tissues compared to healthy tissues.

At the 244th conference of the Electrochemical Society (ECS), Rizwan and his team proposed a broadband monopole antenna for skin cancer detection based on Specific Absorption Rate (SAR) analysis [5]. Their study showed that the SAR of the malignant tissue decreased by almost 0.029 W/Kg compared to the SAR of the healthy tissue.

In her thesis, Katbay proposed a Hilbert Fractal Antenna (HFA) to detect breast cancer based on the variation of the resonant frequency of the antenna on the breast [6]. The simulation of the S11 parameter of her proposed antenna showed 3.5 and 2.2% shift in the resonant frequency of the malignant tissue compared to the healthy tissue.

Several experimental protocols are implemented in the literature to validate the mathematical results (theory, simulation) obtained when designing the antennas used on human tissues. These protocols can be divided into two groups: in vitro and in vivo measurements.

In-vitro experiments consist of reconstructing the characteristics of human tissue from a chemical mixture (mimicking human phantom tissues) or using the flesh of animals whose dielectric properties are like those of human tissues. The products most used in vitro experimentation are ballistic gels [7], medical serums [8], and chemical mixtures based on salt, sugar, and various proportions of other ingredients [9, 10]. However, the best alternative to imitating human tissue is the use of the flesh of certain animals. The meat of pigs is widely used, as can be seen in [11, 12].

In-vivo experimentation allows one to get into the real conditions of human tissues, but the manipulation of sick tissues can pose risks for the manipulator. Moreover, ethical issues require long steps to work on sick subjects. To alleviate these constraints, some studies have used healthy subjects, on whom

* Corresponding authors: Dozohoua Silue (silue.dozohoua@supcom.tn).

they have mimicked the conditions of cancer tumor patients. For example, in [13], to detect a melanoma at 77 GHz, the authors used a dry hand and a wet hand. The difference in permittivity between wet and dry skins mimics that between dry skin and a tumor.

In-vivo validation can also be done on certain live animals, such as pigs and rats. However for the diagnosis of cancer tumors, it is difficult to use these animals because it is necessary to find an animal subject with the same pathology.

Beyond the introductory section, the rest of this paper consists of six parts. Section 2 describes the structure of the proposed antenna and explains the diagnostic method. Section 3 compares the performance of the proposed antenna with that described in the literature. Section 4 presents the performance of the prototype antenna, and Section 5 analyzes the Specific Absorption Rate. In Section 6, a link budget is carried out to determine the range of the signal, and Section 6 concludes the study. It also indicates the future direction of this research work.

2. DESIGN AND METHODOLOGY

2.1. Antenna Structure

In this study, we propose a meander antenna for the early diagnosis of skin sarcoma. The structure of the antenna is inspired by the one presented in the articles [14, 15]. It mainly consists of a thin layer of copper etched on FR-4 with 1.6 mm thickness. Table 1 contains the components of the antenna with their respective dimensions. The use of the proposed antenna involves placing it on the skin of the area under investigation and measuring the resonance frequency. The stage of the tumor is finally defined from the scale of the cancer tumor stage (Fig. 6).

To simulate the antenna parameters in the presence of the human body, a three-layer phantom (skin, fat, muscle) was used. This model was used because it is considered in several studies to be the closest to the reality of the human body [6, 16]. In this study, we consider the muscle, fat, and skin, with thicknesses of 27.5 mm, 8.5 mm, and 2.5 mm, respectively. Fig. 1 shows the geometry of the antenna spread out and placed on the 3-layer model and its dimensions. The sizes of other components are given in Tables 1 and 2, respectively. All sizes are expressed in terms of the free space wavelength (λ_0).

TABLE 1. Detailed antenna sizes.

Dimensions	Sizes in wavelength	Values (mm)
L	$0.215\lambda_0$	31.3
W	$0.107\lambda_0$	15.65
$L1$, $L2$	$0.037\lambda_0$	5.34
$S1$, $S2$	$0.039\lambda_0$	5.71
C	$0.044\lambda_0$	6.4
D	$0.015\lambda_0$	2.19

Our goal is to use the antenna to diagnose skin sarcoma at an early stage. The embryonic state of the tumor is considered in this study to be the time when a surface area of 15.7 mm^2 of the hypodermis changes electrical characteristics.

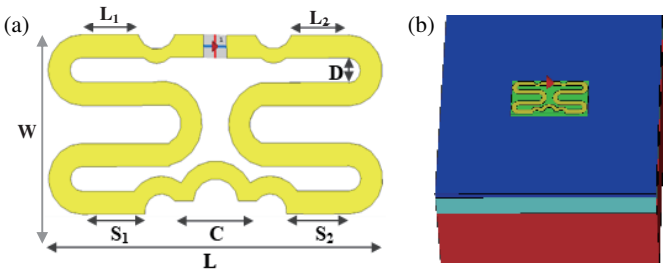

FIGURE 1. Antenna geometry: (a) spread antenna, (b) profile view of the antenna on the 3-layer phantom.

To mimic the behavior of the antenna, the tumor was modeled by a hemisphere placed on the upper surface of the fat. As a malignant tumor is a stack of dead cells with accumulated water, its electrical characteristics are therefore higher than those of normal skin cells. Fig. 2 provides a longitudinal view of the tumor modeled in the embryonic state, and Table 3 summarizes the characteristics of the tissues [17].

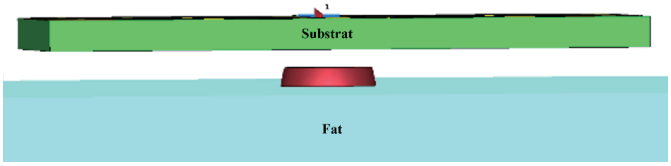

FIGURE 2. Longitudinal view of the tumor, modeled in the embryonic state (the skin is transparent).

2.2. Parametric Equations

It is important to understand the theoretical functioning of the proposed antenna. This helps to choose the appropriate parameters for the expected resonant frequency.

In free space, resonant frequency is mainly a function of substrate permittivity and antenna dimensions. Eq. (1) is used to calculate the free space wavelength λ_0.

$$\lambda_0 = \frac{2\delta_1 L}{0.699h}\sqrt{\frac{\varepsilon_r + 1}{2}} \tag{1}$$

where L is the length of the antenna, and ε_r and h are the relative permittivity and thickness of the substrate, respectively. δ_1 is the thickness of the superstrate.

However, when the antenna is placed on the body, the surrounding tissues combine with the substrate to give an effective permittivity that affects the antenna's resonance. The resonant frequency drops. It is as if the edges of the antenna were stretching. The resonance frequency (f_g) will be calculated using Eq. (2), inspired from the general equations of rectangular patch antennas.

$$\lambda_g = 0.1271\frac{(0.1\delta_2 + 1.818)(\delta_1 + 0.0051)L}{h} \sqrt{\left(\sqrt{\varepsilon_t + 1} + \sqrt{\varepsilon_r + 1}\right)(\varepsilon_r + 1)} \tag{2}$$

where λ_g is the guided wavelength; ε_t and δ_2 are the skin relative permittivity and its thickness; c is the wave celebrity.

TABLE 2. Antenna components dimensions.

Components	Materials	Area ($L \times W$)	Area [mm^2]	Thickness [mm]
Substrate	FR-4	$0.215\lambda_0 \times 0.107\lambda_0$	31.3×15.65	1.6
Superstrate	FR-4			1.6
Radiating element	Cooper			0.035

TABLE 3. Characteristics of tissues.

Charact.Tissues	ε_r	σ [S/m]	ρ [Kg/m^3]	Thickness/Sizes [mm]
Skin	44.62	1.04	1100	2.5
Fat	5.35	0.06	910	8.5
Muscle	54.11	1.14	1041	27.5
Tumor	51.02	4.84	1100	1

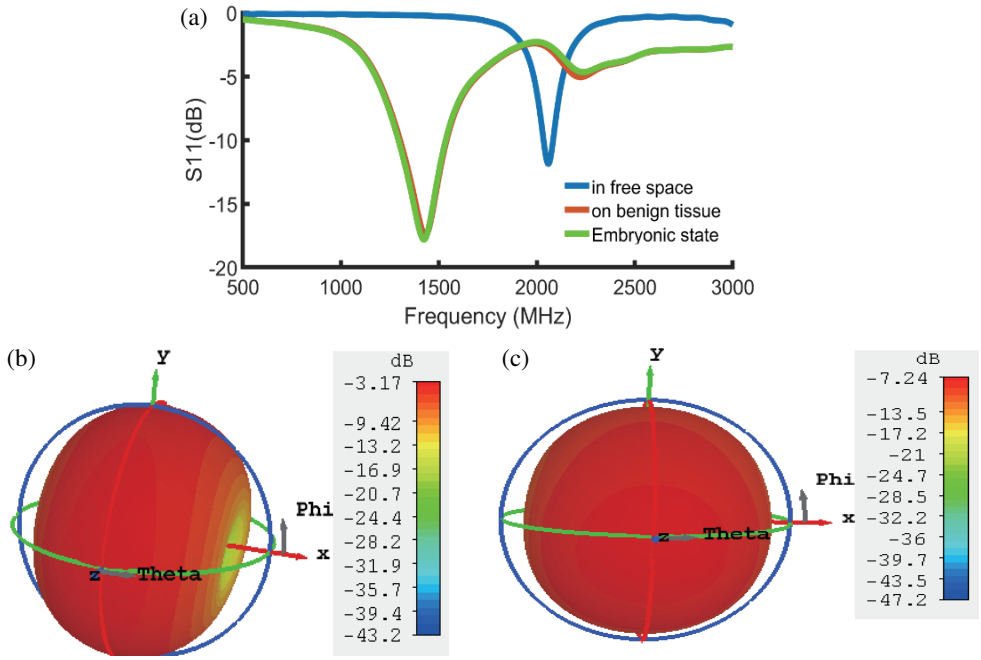

FIGURE 3. Antenna performances: (a) reflection coefficients, (b) realized gain in free space, (c) on benign tissue.

Equation (2) shows that several factors influence the antenna resonance. The proposed antenna design was therefore a compromise between the constraints of the equipment available in the laboratory and that of the propagation medium (tissues).

2.3. Antenna Performance Simulation and Results

Antenna performances were simulated in free space, then in the presence of healthy tissue, and finally when placed on tissue affected by a tumor in the embryonic state. Fig. 3 presents the results of these simulations.

In free space, the antenna resonates at 2057.5 MHz with a reflection coefficient of -11.87 dB and a realized gain of -3.17 dBi. On the healthy tissue and on the affected one, it resonates, respectively, at 1430 MHz and 1422.5 MHz with reflection coefficients of -17.46 dB and -17.81 dB. The realized gain drops from -3.17 dBi to -7.24 dBi and then to -7.3 dBi. The presence of the tumor drops the resonance frequency by 7.5 MHz.

2.4. Tumor Detection in Invasive and Metastasis States

Diseased cells can multiply and spread in the same tissue, which is called invasive cancer. Skin sarcoma, which arises in the hypodermis, can be considered invasive if it spreads into the hypodermis and dermis in both width and thickness. To simulate the reflection coefficient in the invasive state, we considered a half-sphere with a base diameter ranging from 5 mm to 20 mm and a thickness ranging from 1 mm to 1.5 mm. A thickness of 0.01 mm corresponds to a layer of cells.

Contaminated cells can also merge and evolve to contaminate all cells on a localized surface of the hypodermis and even reach the cells of the epidermis. In this case, it is said that the cancer is in a state of metastasis. In the case of this study, in the

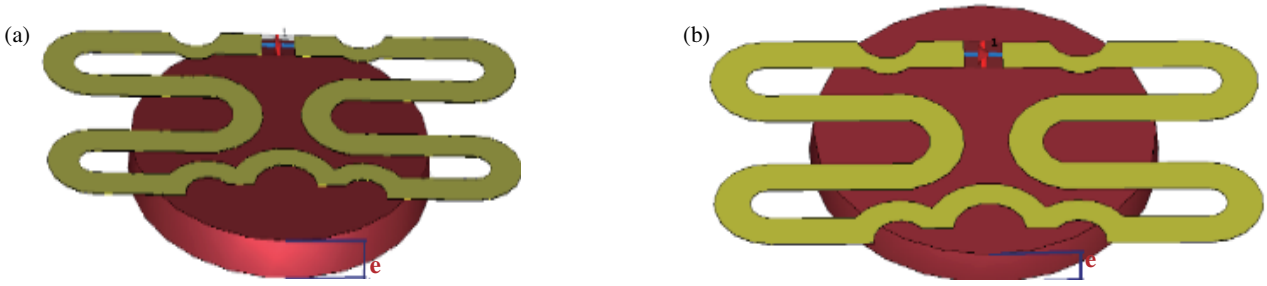

FIGURE 4. Modeling of the tumor: (a) invasive state, (b) metastasis state (all tissues were made transparent). (a) $D = 20\,\text{mm}$, $e = 1.5\,\text{mm}$, (b) $D = 20\,\text{mm}$, $e = 2\,\text{mm}$.

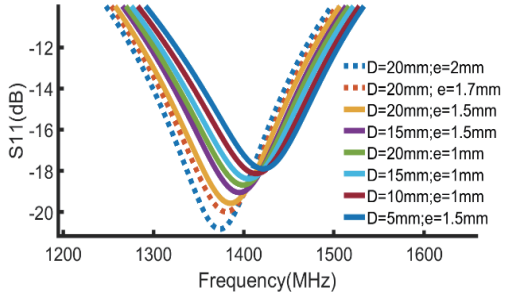

FIGURE 5. Reflection coefficients in invasive and metastasis state.

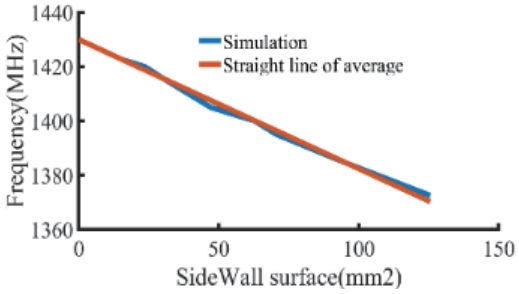

FIGURE 6. Scale for tumor lateral surface prediction.

state of metastasis of the sarcoma, the set of dead cells is modeled by a half-sphere of thickness ranging from 1.5 to 2 mm and a central diameter of 20 mm. This diameter corresponds to the size that a skin tumor can reach. The modeled tumor in the terminal invasive and metastasis phases is presented in Fig. 4, and in Fig. 5 the variations of resonance frequency are presented.

Figure 5 shows the variation of the reflection coefficient during tumor growth in the invasive and metastasis phases.

In the presence of a metastasis tumor, resonances are obtained at frequencies of 1380 MHz and 1372.5 MHz for tumors with thickness of 1.7 mm and 2 mm, respectively. The observed reflection coefficients are -20 dB and -20.85 dB.

This study confirms that the presence of a cancerous tumor causes a fall in resonance frequency relative to the resonant frequencies of the same antenna in healthy tissue. The variation reached 57.5 MHz for tumors with metastases of 125.6 mm^2. This result is consistent with the 50 MHz resonance frequency variation observed in [6] for a side surface of 100 mm^2 (a cube of 5 mm). Furthermore, the minor difference between our results and those observed in [6] can be explained by the type of tissue. Our work considered the skin of flat organs such as the arm, forearm, back, and thighs, while the referenced work involved the breast.

2.5. Prediction Scale for the Lateral Surface of the Tumor

We calculated the volume and lateral surface of the tumor at each phase of its evolution. The lateral surface and volume analysis in relation to the evolution of the resonance frequencies shows that the resonance evolves according to the lateral surface of the tumor and not its volume (Fig. 6). This is a significant observation that can help surgeons determine the tumor extent during surgical interventions. In view of the results obtained, we have established Table 4, to serve as a reference in the diagnosis of skin sarcoma.

The variation in resonance frequency depending on the lateral surface of the tumor is an affine decreasing function (Eq. (3)).

$$f(x) = ax + 1429.97 \tag{3}$$

with f being the resonance frequency in MHz and x the side surface in mm^2. The inclination a of this equation is -0.4757 MHz/mm^2. It represents the falling coefficient of resonance frequency per 1 mm^2 of cancer tumor surface. This variation is consistent with the 50 MHz drop observed in [10] for a cubic tumor of 5 mm of size and side surface equal to 100 mm^2.

3. COMPARISON OF THE RESULTS WITH PUBLISHED DATA

The performance of the proposed antenna is compared in Table 5 with those obtained in recent works. To our knowledge, the proposed method is the only one that gives a clear protocol that allows all practitioners to use it.

It is safe to assume that the proposed antenna is smaller than the most usual antennas while resonating in a much lower frequency band (1430 MHz). In addition, our antenna detects cancerous tumors at an earlier stage than other antennas.

The originality of the proposed diagnosis method lies in the ease of use of the diagnostic method, based on a scale and a table of reference values. The study also makes it possible to accurately determine tumor size, which will help surgeons make precise incisions during medical procedures.

TABLE 4. Scale of cancer tumor stage.

Resonance frequency F_0 [MHz]	Characteristics of the tumor		
	Depth (h) of tumor (mm)	Tumor states	Observations
1430	0	No Tumor	Normal skin
1422.5	1	Embryonic stage	Invisible to the naked eye, cannot be perceived by palpation, detection by the antenna resonance with specified size.
$1422.5 \leq F_0 < 1385$	$1 < h < 1.5$	First step of Invasive state	Detectable by finger pressure without tumor size determination, detection by resonance shift with size determination.
$1380 \leq F_0 < 1385$	$1.5 \leq h < 1.7$	Second step of Invasive state	Appearance of balls, can be perceived by touch without size determination, detection by resonance shift with specified size.
$1372.5 \leq F_0 < 1380$	$1.7 \leq h \leq 2$	Metastasis	Cancer spread in the dermis, Visible by inspection

FIGURE 7. Measurement: (a) antenna prototype, (b) experimental setup, (c) reflection coefficient on benign tissue.

4. STEPS OF THE MEASURES

A prototype of the antenna (Fig. 7(a)) was made on an FR-4 type substrate using the laboratory LPKF milling machine.

The measurements were carried out with the Agilent 8714ES Vector Network Analyzer (VNA) as illustrated in Figs. 7(b) and 7(c), first in open space, then in vivo on various healthy skins and on skins reinforced with a sodium and sugar solution.

The measurement of the in vivo reflection coefficient on healthy skin consisted in placing the antenna on the skin of different organs (front and back of the shoulder and thigh) of three individuals. To mimic the dielectric properties of malignant skin, a solution composed of 500 ml of water, 76.5 g of sodium, and 23.5 g of sugar [22] was deposited on an area of $11.2 \times 11.2\,\text{mm}^2$ of the skin of each healthy subject. The deposition of the solution results in a slight increase in the permittivity and conductivity of the skin over the $125.44\,\text{mm}^2$, corresponding to the final phase of the tumor metastatic state. The results of those measurements are compared with the simulation results (Fig. 8).

4.1. Results of the Reflection Coefficient

In free space (Fig. 8(a)), the antenna prototype resonates at a frequency of 2014.167 MHz with a tolerance of 0.1% and presents a reflection coefficient of -22.219 dB with a measured bandwidth of 69.18 MHz.

Measurements on the healthy skin of three different individuals (2 men, 1 woman) and on three different organs (the forearm, back of the neck, and thigh) showed that the antenna resonates at a frequency of 1430 MHz with different values of the reflection coefficient. Furthermore, the best fit is obtained on the forearm of a 42-year-old man of 71 kg and 171 cm height, where the reflection coefficient reaches -26.576 dB. The bandwidth is 207.8 MHz. Given the low weight of the antenna, the fluctuation of the resonant frequency of the antenna on the skin reaches 0.1% compared to the value of the simulation.

In the presence of a tumor in its final metastasis state, the measurements showed that the antenna resonates at a frequency of 1372.5 MHz with a reflection coefficient of -28.259 dB. The measured bandwidth of the antenna under these conditions is 245 MHz. From the analysis of these results, it can be stated that the results obtained by simulations and those obtained by measurements agree perfectly.

TABLE 5. Performance comparison table.

Ref.	Antenna sizes (mm^3)	Resonance frequency (GHz)	Characteristics of the tumor				Methods of diagnosis
			Organ	Vol. (mm^3)	ε_r	σ (m)	
[5]	$20 \times 28 \times 1.6$	2.81	Skin	65.41	51.2	9.8	Late stage detection by SAR variation (0.029 W/Kg reduction compared to healthy tissue); A single tumor stage.
[6]	$32.4 \times 13.5 \times 1.6$	0.90 2.2	Breast	125	50	4	Late stage detection by resonance frequency shift (2.2–3.5%); A single tumor stage.
[18]	$20 \times 24 \times 1.6$	7.5	Breast	33.49	50	4	Late stage detection by SAR variation (0.9 mW/Kg reduction compared to healthy tissue);
[19]	$10 \times 10 \times 0.375$	8	Breast	32.71	No.	No.	Late stage detection by image reconstruction; A single tumor stage.
[20]	$61 \times 0.411 \times no$	2.4	skin	No.	54.9	4	Early detection by current density, E-field and H-field variation; No details on Timor size and Phantom.
[21]	$40 \times 40 \times 0.15$	8.3	Skin	523.33	32.3	6.9	Detection by decreased impedance matching; Late stage detection.
This work	$31.3 \times 15.65 \times 1.6$	1.430	Skin	26.17	51.02	4.84	Early detection by resonance frequency shift, detection by SAR variation; Measurement of tumor size; Stage since 26.17 mm^3.

TABLE 6. Link budget parameters.

Symbol	Quantity	Value
Pt	Transmitter power [dBm]	-20
Gt	Transmitter antenna gain [dBi]	-7.24
Gr	Receiver antenna gain [dBi]	3.6
L	Free space loss [dB]	-103.79
S	IoT node sensitivity [dBm]	-136
M	Margin	10
n	Path loss exponent	3
Pr	Receiver power [dBm]	$Pr = S + M$
d	Distance between transmitter and receiver [m]	118.90 m at 1430 MHz

5. SPECIFIC ABSORPTION RATE (SAR)

It is important to analyze the power absorbed by tissues for any system radiating close to the body to understand the potential ionization risks of tissues.

Therefore, we generated the power lost in the copper and the power absorbed by the various tissues (skin, fat, and muscle). Fig. 9 shows the distribution of power lost in each tissue. Observation of the power loss density shows that the skin absorbs the maximum power at around 2.5×10^5 W/m^3, i.e., less than 0.227 W/g. This value is well below the maximum value of 1.6 W/g authorized by the American National Standard Institute (ANSI) [23]. It may be noted, however, that the central arcs of the antenna generate the greatest power loss.

6. LINK BUDGET

Today, technology can only be sustainable if it is scalable and easy to use by many users. We therefore wanted to see if the proposed antenna could be implemented in an IoMT (Internet of Medical Things) sensor to establish OB2OB (Out of Body-to Out of Body) communication. The antenna could then be used to transmit measurements directly to a connected Gateway.

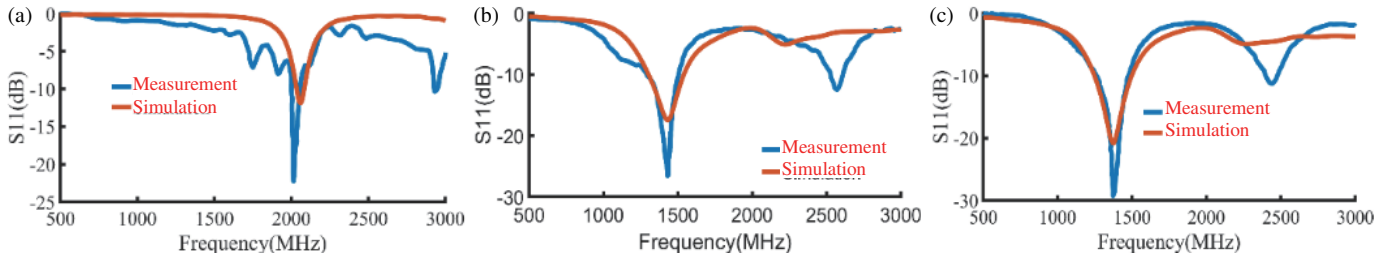

FIGURE 8. Simulated and measurements of reflection coefficient: (a) in free space, (b) benign tissue, (c) on malignant tissue.

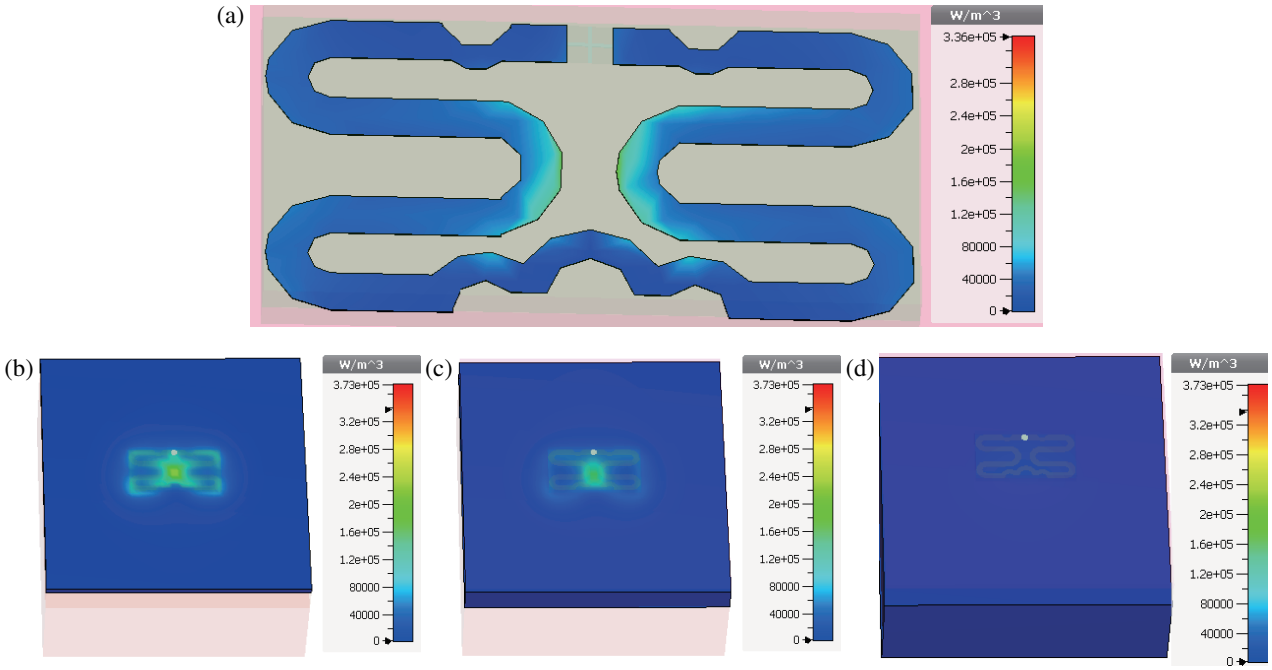

FIGURE 9. Power loss (a) in the copper (b) in the skin, (c) in the fat (d) in the muscle.

To ensure this capability, we have evaluated the range of the signal generated by the antenna when it is excited with a power of −20 dBm. When the antenna is well matched, the range of the signal can be estimated with Eq. (4) from the article [24].

$$P_r[\text{dBm}] = \text{EIRP}[\text{dBm}] + G_r[\text{dBi}] - L[\text{dB}] \tag{4}$$

where

$$\text{EIPR}[\text{dBm}] = P_t[\text{dBm}] + G_t[\text{dBi}] \tag{5}$$

$$L[\text{dB}] = 10n\log(d) + 10\log\left(\frac{4\pi d}{\lambda_0}\right) \tag{6}$$

where EIRP is the Equivalent Isotropic Radiated Power, P_t the transmitted power, G_t our proposed antenna gain at 1430 MHz, and G_r the gain of an IoT node, L is the path loss, and n is the propagation exponent which is 3 in NLOS (None-Line-Of-Sight) situation.

NLOS propagation is the mode of wave propagation in media with obstacles. Obstacles can cause losses in the signal level due to propagation mechanisms (reflection, refraction, diffraction, and absorption). The direct consequence of the loss of the signal level is the decrease of the range of the radio waves.

From Eqs. (4) and (6) we can derive Eq. (7).

$$d = \sqrt[(1+n)]{\frac{\lambda_0}{4\pi} * 10^{\left(\frac{L}{10}\right)}} \tag{7}$$

Table 6 lists the parameters used to calculate the range of the radio-frequency signal.

The range of the wave generated by the proposed antenna can reach 118.90 m in a complex environment when fed with only −20 dBm. This shows that the antenna can equip sensors communicating with an IoT gateway in a large hospital. This antenna is therefore a good candidate for the vulgarization of IoMT.

7. CONCLUSION

In this paper, a miniature antenna for early diagnosis of skin sarcoma is presented. The proposed antenna allows to overcome the constraints of the usual methods of detection of hypodermal cancer tumors at all stages of their evolution. Compared to the antenna performance on the healthy tissue model, the results of the phantom malignant tissue simulation showed a decrease in

the resonance frequency of 7.5 MHz in the presence of a cancer tumor of 26.17 mm^3.

To validate the simulation results, the antenna was manufactured on an FR-4 substrate, and the results of measurements on the affected skin of a tumor at the final state of metastasis confirm the fall in the resonance frequency of 57.5 MHz, and an improvement of -1.683 dB in impedance adaptation. In parallel to cancer detection, the antenna can also be used to establish 118.90 m body links. In future work, we will test the antenna on a significant population.

REFERENCES

[1] FRENCH ARC Foundation, "Skin cancers, information brochure," Jul. 2018, [Online]. Available: https://www.fondation-arc.org.

[2] BELGIAN Cancer Registry, "Cancer burden in Belgium, 2004-2019," 2022, [Online]. https://kankerregister.org/media/docs/publications/Shortreport_Cancerburden_2004-2019.pdf.

[3] Hartinger, A., "Detection of skin cancer by electrical impedance tomography," Ph.D. dissertation, Dept. Biomed. Eng., Eng. Univ.-Polyt., Montréal, Quebec, 2012.

[4] Joines, W., Y. Zhang, C. X. Li, and R. L. Jirtle, "The measured electrical-properties of normal and malignant human tissues from 50 to 900 MHz," *Medical Physics*, Vol. 21, No. 4, 547–550, Apr. 1994.

[5] Rizwan, S. and K. V. P. Kumar, "An ultra-wideband monopole antenna for skin cancer detection," in *Journal of Physics: Conference Series*, Vol. 2335, No. 1, IOP Publishing, 012001, 2022.

[6] Katbay, Z., "Development of antennas for the detection of cancerous tumors in the breast," Ph.D. dissertation, Dept, Math. et Sci. et Techn. de l'Inform. et de la Comm., Univ. de Bret. Occid. Comue Univ. Bret. Loire et de l'Univ. Lib., Liban, 2018.

[7] Sharma, D., B. K. Kanaujia, V. Kaim, R. Mittra, R. K. Arya, and L. Matekovits, "Design and implementation of compact dual-band conformal antenna for leadless cardiac pacemaker system," *Scientific Reports*, Vol. 12, No. 1, Feb. 24, 2022.

[8] Alwan, M., S. Sadek, and Z. Katbay, "Investigation of tumor using an antenna scanning system mohamad," in *Proceedings of 2014 Mediterranean Microwave Symposium (MMS 2014)*, 216–219, Dec. 12-14, 2014.

[9] Cheng, X., J. Wu, R. Blank, D. E. Senior, and Y.-K. Yoon, "An omnidirectional wrappable compact patch antenna for wireless endoscope applications," *IEEE Antennas and Wireless Propagation Letters*, Vol. 11, 1667–1670, 2012.

[10] Narmadha, G., M. Malathi, S. A. Kumar, T. Shanmuganantham, and S. Deivasigamani, "Performance of implantable antenna at ISM band characteristics for biomedical base," *ICT Express*, Vol. 8, No. 2, 198–201, Jun. 2022.

[11] Alrawashdeh, R. S., Y. Huang, M. Kod, and A. A. B. Sajak, "A broadband flexible implantable loop antenna with complementary split ring resonators," *IEEE Antennas and Wireless Propagation Letters*, Vol. 14, 1506–1509, 2015.

[12] Kod, M., J. Zhou, Y. Huang, M. Stanley, M. N. Hussein, A. P. Sohrab, R. Alrawashdeh, and G. Wang, "Feasibility study of using the housing cases of implantable devices as antennas," *IEEE Access*, Vol. 4, 6939–6949, 2016.

[13] Arab, H., L. Chioukh, M. D. Ardakani, S. Dufour, and S. O. Tatu, "Early-stage detection of melanoma skin cancer using contactless millimeter-wave sensors," *IEEE Sensors Journal*, Vol. 20, No. 13, 7310–7317, Jul. 1, 2020.

[14] Alrawashdeh, R., Y. Huang, and P. Cao, "Flexible meandered loop antenna for implants in medradio and ISM bands," *Electronics Letters*, Vol. 49, No. 24, 1515–1516, Nov. 21, 2013.

[15] Silue, D., F. Choubani, and M. Labidi, "Enhanced meander antenna for in-body telemetry applications," in *2022 18th International Conference on Wireless and Mobile Computing, Networking and Communications (wimob)*, Oct. 10-12, 2022.

[16] Krimi, I., S. Ben Mbarek, S. Amara, F. Choubani, and Y. Massoud, "Mathematical channel modeling of electromagnetic waves in biological tissues for wireless body communication," *Electronics*, Vol. 12, No. 6, Mar. 2023.

[17] Carrara, N., "Dielectric properties of body tissues," 2007. [Online]. Available: http://niremf.ifac.cnr.it/tissprop/

[18] Brinda, K., K. P. Sandeep, N. Priyadharshini, K. C. Sree, and R. Agarwal, "Design of ultra-wideband planar monopole antenna for breast tumor detection," in *2019 International Conference on Vision Towards Emerging Trends in Communication and Networking (ViTECoN)*, 1–4, 2019.

[19] Saeidi, T., S. N. Mahmood, A. J. Ishak, S. Alani, S. M. Ali, I. Ismail, and A. R. Alhawari, "Miniaturized spiral UWB transparent wearable flexible antenna for breast cancer detection," in *2020 International Symposium on Networks, Computers and Communications (ISNCC)*, 1–6, 2020.

[20] Karthikeyan, T. A., M. Nesasudha, and G. S. Deepthy, "Early detection of skin tumor using dipole antenna," in *ICSPC'21: 2021 3rd International Conference on Signal Processing and Communication (ICPSC)*, 412–416, May 13-14, 2021.

[21] Kaur, K. and A. Kaur, "Fractal geometry based CPW fed antenna for early stage Skin cancer detection," in *2021 IEEE Indian Conference on Antennas and Propagation (InCAP)*, 517–520, 2021.

[22] GUY, A., "Analyses of electromagnetic fields induced in biological tissues by thermographic studies on equivalent phantom models," *IEEE Transactions on Microwave Theory and Techniques*, Vol. MT19, No. 2, 205, 1971.

[23] IEEE C95. 1, "IEEE standard for safety levels with respect to human exposure to electric, magnetic and electromagnetic fields, 0 Hz to 300 GHz," *The Institute of Electrical and Electronics Engineers*, 2019.

[24] Silue, D. and F. Choubani, "Small antenna for leads pacemakers," in *2022 IEEE Ninth International Conference on Communications and Networking (COMNET)*, 1–5, 2022.